Expansion of CD14^{+}HLA-DR$^{neg/low}$ monocytes and CD10^{neg} neutrophils driving proinflammatory responses in patients with acute myocardial infarction

Daniela Fraccarollo[1*], Jonas Neuser[1], Julian Möller[1], Paolo Galuppo[1], Johann Bauersachs[1]

[1]Department of Cardiology and Angiology, Hannover Medical School, Hannover, Germany

Author Notes

Daniela Fraccarollo and Jonas Neuser are co–first authors.

Paolo Galuppo and Johann Bauersachs are co–senior authors.

Fraccarollo et al.: HLA-DR$^{neg/low}$ monocytes/CD10^{neg} neutrophils in AMI

[*]Corresponding author:

Dr. Daniela Fraccarollo
Department of Cardiology and Angiology
Medical School Hannover
Carl-Neuberg-Str.1
30625 Hannover, Germany
Phone: (+49) 5115325773
Fax: (+49) 5115328194
e-mail: fraccarollo.daniela@mh-hannover.de

ABSTRACT

Background

Immature myeloid cells expand in cancer, autoimmune diseases and viral infection, but their appearance and function after acute myocardial infarction (AMI) remain underexplored.

Methods and Result

Using flow cytometry, cell sorting and a mouse model of ischemia/reperfusion we investigated the role of immature granulocytic/monocytic cells in immune responses post-AMI. Seventy-one patients were categorized into unstable angina (n=11), Non-ST-elevation MI (NSTEMI, n=16), and ST-elevation MI (STEMI, n=44). Circulating $CD14^{+}HLA\text{-}DR^{neg/low}$ monocytes and normal-density $CD16^{+}CD66b^{+}CD10^{neg}$ neutrophils are expanded in patients with large AMI and strongly correlated with cardiac damage, function and serum levels of S100A9/S100A8, MMP-9 and IL-1ß. Receiver operating characteristic curve analysis highlighted ability of $CD14^{+}HLA\text{-}DR^{neg/low}$ and $CD16^{+}CD66b^{+}CD10^{neg}$ cells in discriminating acute coronary syndromes. $CD14^{+}HLA\text{-}DR^{neg/low}$ monocytes did not suppress T-cell proliferation but expressed high amounts of IL1R1 and S100A9. Mechanistically, macrophages differentiated from $CD14^{+}HLA\text{-}DR^{neg/low}$ monocytes produced more proinflammatory cytokines upon IFNγ stimulation as $CD14^{+}HLA\text{-}DR^{high}$ monocyte-derived macrophages. $CD10^{neg}$ neutrophils expressed MMP9 and S100A9 at higher levels compared to $CD10^{pos}$ neutrophils. IFNγ production by $CD4^{+}$ T-cells was increased in presence of $CD10^{neg}$ neutrophils. Remarkably, elevated circulating IFNγ levels were detected in cytomegalovirus-seropositive patients with expanded $CD10^{neg}$ neutrophils and increased frequency of $CD4^{+}CD28^{null}$ T-cells. Lastly, we showed that murine homologs of human $CD10^{neg}$ neutrophils are $Ly6G^{pos}CXCR2^{pos}CD11b^{dim}CD101^{neg}$ cells. $CD101^{neg}$ neutrophils are rapidly released into the bloodstream after AMI and migrate to ischemic sites, displaying increased expression of MMP-9 at 3 hours and of IL-1ß at 24 hours after reperfusion.

Conclusion

$CD14^{+}HLA\text{-}DR^{neg/low}$ monocytes and normal-density $CD10^{neg}$ neutrophils inducing proinflammatory immune responses expand in patients with AMI.

INTRODUCTION

Despite advances in interventional therapies patients with large acute myocardial infarction (AMI) are at higher risk of heart failure morbidity and mortality.[1] Immunity and inflammation play a key role in the pathogenesis of ischemic heart failure and the complex role of immune cells during the wound healing process after injury is currently the focus of intensive research efforts. Understanding the immune mechanisms operating during AMI could pave the way to develop more effective strategies to prevent progressive dilative cardiac remodeling, functional deterioration and heart failure and to reduce cardiovascular adverse events.

HLA-DR$^{neg/low}$ monocytes and CD10^{neg} neutrophils expand in pathological conditions such as cancer, infection and inflammation,[2] and have recently been implicated in the pathogenesis of severe COVID-19,[3-4] but their role in immunoregulatory mechanisms operating during AMI remains largely unknown.

By integrating flow cytometry, cell sorting, and *in vitro* experiments this study investigated the appearance and function of HLA-DR$^{neg/low}$ monocytes and normal-density CD10^{neg} neutrophils in patients with AMI. We explored whether increased frequencies of HLA-DR$^{neg/low}$ monocytes and CD10^{neg} neutrophils are linked to circulating levels of G-CSF, S100A9/S100A8, MMP-9, NGAL, MPO, IL-6, TNFα and IL-1ß, immune regulators and acute inflammation markers. Moreover, we performed flow cytometric immunophenotyping of lymphocyte subsets and investigated circulating levels of IFNγ.

We found that CD14^{+}HLA-DR$^{neg/low}$ monocytes are not immunosuppressive but secrete high levels of TNFα, IL-6, and IL-1ß after differentiation to macrophages and IFNγ stimulation. Further, our results point to a potential link among increased frequency of normal-density CD10^{neg} neutrophils, circulating CD4^{+}CD28^{null} T-cells and elevated IFNγ levels, especially in cytomegalovirus-seropositive patients. Lastly, using a mouse model of ischemia/reperfusion we showed that cardiac injury was associated with expansion of immature Ly6G^{pos}CXCR2^{pos}CD11b^{dim}CD101^{neg} cells in circulating blood and that immature neutrophils are a major source of MMP-9 and IL-1ß in the ischemic reperfused myocardium.

Methods

Patients and Study Design

The study protocol is in accordance with the ethical guidelines of the 1975 declaration of Helsinki and has been approved by the local ethics committee of Hannover Medical School. Patient referred to your clinic for acute coronary syndrome (ACS) were included after providing written informed consent. Patients suffering from active malignant diseases or receiving immunosuppressive therapy were not included. Seventy-one patients (Table 1) were categorized into unstable angina (n=11), Non-ST-elevation MI (NSTEMI, n=16), and ST-elevation MI (STEMI, n=44). Left ventricular ejection fraction (LVEF) was measured in 2D echocardiographic studies using bi-plane Simpson's method. Seventeen healthy volunteers were recruited as control subjects.

Flow cytometry

Venous blood was collected in EDTA tubes, stored at room temperature and processed within 1 hour of collection. White blood cell count was measured by an automated hematology analyzer (XT 2000i, Sysmex). Serum was separated within 45 minutes and stored at −80°C. For multiparameter flow cytometry whole blood (100µL) was incubated with fluorochrome-conjugated antibodies for 30 minutes at room temperature in the dark, followed by lysis of red blood cells with Versalyse Lysing Solution® (Beckman Coulter).[5] Finally, the cells were washed twice with Hanks buffer (4 mL). For cell sorting by flow cytometry cells were resuspended in ice-cold FACS-staining buffer (PBS, supplemented with 0.5% bovine serum albumin and 2mM EDTA) and immunostaining was performed on ice. The following antibodies were used: anti-CD14 (Clone M5E2, 1:50 BD Biosciences); anti HLA-DR (Clone L243, 1:30 BioLegend); anti-CD16 (Clone 3G8, 1:50 BioLegend); anti-CX3CR1 (Clone 2A9-1, 1:50 BioLegend); anti-CCR2 (Clone K036C2, 1:50 BioLegend); anti-CD66 (Clone G10F5, 1:30 BioLegend); anti-CD10 (Clone HI10a, 1:20 BioLegend); anti-CD3 (Clone SK7, 1:30 BD Biosciences); anti-CD4 (Clone RPA-T4, 1:30 BD Biosciences); anti-CD28 (Clone CD28.2, 1:30 BioLegend); anti-CCR7 (Clone G043H7, 1:30 BioLegend); anti-CD45RO (Clone UCHL1, 1:30 BioLegend). Fluorescence minus one (FMO) controls were included during acquisition for gating analyses to distinguish positive from negative staining cell populations. FACS data were acquired on a GalliosTM flow cytometer and analyzed with GalliosTM software (Beckman Coulter).

Isolation of blood mononuclear cells and neutrophils

Peripheral blood was collected in EDTA tubes and mononuclear cells (PBMC) were isolated by density gradient centrifugation using Ficoll®-Paque Premium (GE Healthcare

Biosciences). $CD14^{+}HLA\text{-}DR^{neg/low}$/CD14+$HLA\text{-}DR^{high}$ monocytes cells were FACS-sorted from PBMC. Granulocytes/neutrophils were isolated from the erythrocyte fraction by dextran sedimentation or from whole blood by immunomagnetic selection (130-104-434, MACSxpress® Whole Blood Neutrophil Isolation Kit; Miltenyi Biotec), and $CD10^{neg}$/$CD10^{pos}$ neutrophils were separated by flow-cytometric sorting. Cells were sorted in RTL Lysis Buffer plus 1% β-mercaptoethanol (74134, RNeasy Plus Mini Kit; QIAGEN), or in sterile Sorting Medium [RPMI 1640 supplemented with 10% (v/v) Heat-Inactivated Fetal Bovine Serum (HI-FCS; A3840001; Gibco)]. Cell sorting was performed using a FACS Aria Fusion or FACS Aria IIu (BD Biosciences).

Macrophage generation and stimulation

For in vitro differentiation of monocytes into macrophages, FACS-sorted cells were suspended at 0.5×10^{6} cells/mL in RPMI 1640 medium supplemented with 10% HI-FCS and 1% PenStrep (10378016; Gibco). $CD14^{+}HLA\text{-}DR^{neg/low}$/$CD14^{+}HLA\text{-}DR^{high}$ monocytes were cultured in 96 well plates (200µL/well) in the presence of 20 ng/mL M-CSF (216-MC-005; R&D Systems) for 4 days.[6] Monocyte-derived macrophages [(Mb), in RPMI 1640 medium supplemented with 2% HI-FCS] were stimulated with 20 ng/mL of IFNγ [M(IFNγ), 285-IF; R&D Systems] for 48 hours.

T-cell activation assays in presence of monocytes

Isolation of $CD3^{+}$ T-cells was performed using Dynabeads® Untouched™ Human T-cells Kit (11344D, Invitrogen). $CD3^{+}$ T-cells were stained with CellTrace Violet Cell Proliferation Kit (C34571; Invitrogen) and resuspended at $1x10^{6}$/mL in OpTmizer™ CTS™ T-Cell Expansion culture medium supplemented with L-glutamine/PenStrep (A1048501; Gibco). $CD3^{+}$ T-cells were co-cultured in 96 well plates with $CD14^{+}HLA\text{-}DR^{neg/low}$ and $CD14^{+}HLA\text{-}DR^{high}$ monocytes at a ratio of 1 to 1 (T-cells: monocytes). T-cells were stimulated with Dynabeads Human T-Activator CD3/CD28 (11131D; Gibco) and T-cell proliferation was assessed 4 days later by CellTrace™ Violet dilution by flow cytometry.

T-cell activation assays in presence of $CD10^{neg}$/$CD10^{pos}$ neutrophils

$CD4^{+}$ T-cells were isolated from PBMC using the MojoSort™ Human CD4 T Cell Isolation Kit (480009; BioLegend) or by flow-cytometric sorting. $CD4^{+}$ T-cells were resuspended at $1x10^{6}$/mL in OpTmizer™ CTS™ T-Cell Expansion culture medium supplemented with L-glutamine/PenStrep and were activated with Dynabeads Human T-Activator CD3/CD28. For transwell experiments $CD4^{+}$ T-cells and $CD10^{neg}$/$CD10^{pos}$ neutrophils were co-cultured in 24 well plates at a ratio of 1 to 2 (T-cells: neutrophils) for 48 hours. $CD10^{neg}$/$CD10^{pos}$ neutrophils

were cultured in 0.4-µm transwell inserts (140620, Thermo Scientific™) and $CD4^+$ T-cells in the well beneath the insert.

LEGENDplex and ELISA assays

Blood levels of G-CSF, MMP9, S100A9/S100A8, NGAL, MPO, TNFα, IL-6, IL-1ß and IFNγ were measured using bead-based multiplex assays (740180; 740589; 740929; LEGENDplex™ BioLegend). Serum samples were screened for CMV-specific IgG antibodies with the CMV-IgG-ELISA PKS medac enzyme immunoassay (115-Q-PKS; Medac Diagnostika). Levels of IFNγ, TNFα, IL-6, and IL-1ß in the cell-culture supernatants were measured by ELISA (DIF50; R&D Systems) and using bead-based immunoassay (740929; LEGENDplex™ BioLegend).

RT-quantitative PCR

RNA was isolated from cells sorted in RTL Lysis Buffer using the RNeasy Plus Mini Kit (QIAGEN) according to the manufactures' protocol. RNA quantification and quality testing were assessed by NanoDrop 2000 (Thermo Fisher Scientific) and Bioanalyzer 2100 (Agilent). cDNA synthesis was performed using 3 ng (neutrophils) and 10 ng (monocytes) of total RNA and iScriptTM Reverse Transcription Supermix (Bio-Rad). Relative quantitation of mRNA expression levels was determined with CFX96 TouchTM Real Time PCR using SsoAdvancedTM Universal SYBR Green Supermix and PrimePCRTM Primers (Bio-Rad). ß-actin (ACTB) was chosen as an endogenous control. PCR amplification was performed at initially 95 °C for 30 s followed by 40 cycles at 95 °C for 5 s and terminated by 60 °C for 30 s. The delta-delta Ct method was employed for data analysis.

An expanded Methods section is available in the online-only Data Supplement.

Statistical Analysis

Data are presented as mean ± SEM, SD or as median [interquartile range] as indicated. Normality of data was assessed by Shapiro-Wilk test. Non-parametric data from two independent groups were compared using Mann-Whitney *U* test and for more than two groups using Kruskal-Wallis test. Normal data were analyzed by one-way ANOVA with Tukey *post hoc* test. Pearson's *r* was used to test for correlation between two variables. Values of $P \leq 0.05$ were considered statistically significant.

RESULTS

Increased circulating levels of CD14^{+}HLA-DR$^{neg/low}$ monocytes in patients with acute MI.

Phenotypic characterization of monocytes and neutrophils was performed in whole blood from patients with unstable angina (UA) or acute MI within 24 to 72 hours of symptom onset (median 43.6 hours). A time-course analysis within the initial 24 hours and up to day 5 after MI is shown in Figure I in the online-only Data Supplement.

NSTEMI/STEMI patients displayed significantly higher absolute neutrophil and monocyte counts versus UA patients (Table 2). Based on HLA-DR/CD14 expression monocytes can be divided into different subsets. We detected increased circulating levels of intermediate (HLA-DR^{++}CD14^{++}CD16^{+}CX3CR1^{+}) in ACS patients versus control, and of non-classical (HLA-DR^{+}CD14^{+}CD16^{++}CX3CR1^{++}) in STEMI versus UA patients (Table 2 and Figure II in the online-only Data Supplement). There were no significant correlations between intermediate/non-classical monocytes and LV ejection fraction/CK_{max}.

We found increased frequencies of CD14^{+}HLA-DR$^{neg/low}$ monocytes in STEMI patients as compared to UA patients (Figure 1A, 1B and Table 2). Receiver operating characteristic (ROC) curve analysis based on CD14^{+}HLA-DR$^{neg/low}$ monocyte frequencies, discriminating STEMI and UA patients revealed an AUC of 0.904 (95% CI: 0.817-0.991; P<0.01) whereas a lower AUC discriminating NSTEMI and UA patients was observed (AUC=0.7472; 95% CI: 0.558-0.935; P<0.01). By combining CD14^{+}HLA-DR$^{neg/low}$ monocytes with CK_{max} AUC was increased to 0.937; (95% CI: 0.873-1) (Figure 1C) but not in combination with LVEF (AUC=0.852; 95% CI: 0.709-0.996) compared to CD14^{+}HLA-DR$^{neg/low}$ monocytes alone discriminating STEMI and UA patients. Linear regression analysis revealed a negative correlation between the frequency of CD14^{+}HLA-DR$^{neg/low}$ monocytes and LVEF, and positive correlations with CK_{max} (Figure 1D).

In a subgroup of patients we measured serum levels of immune inflammation markers (Table 3). MMP-9, S100A9/S100A8, NGAL, IL-6, and IL-1ß levels were higher in STEMI patients versus UA patients. Moreover, frequency of CD14^{+}HLA-DR$^{neg/low}$ cells significantly correlated with circulating levels of MMP-9, S100A9/S100A8, IL-6, IL-1ß, TNFα, MPO, and NGAL (Figure IIIA in the online-only Data Supplement).

Next, we analyzed the immunoregulatory features of CD14^{+}HLA-DR$^{neg/low}$ monocytes. Using FACS-sorting, CD14^{+}HLA-DR$^{neg/low}$/CD14^{+}HLA-DR^{high} cells were isolated from blood of patients with AMI (Figure 2A). Quantitative RT-PCR showed that CD14^{+}HLA-DR$^{neg/low}$ monocytes express high amounts of S100A9 and IL1R1 (Figure 2B). Of interest, studies in

heart failure patients have provided evidence for the presence of HLA-DR$^{neg/low}$ cells within myocardial tissue expressing high levels of S100A9.[7] No difference was seen in the expression of CAT, CCR1, IL1R2, LCN2, MMP8, NOS2, SAAP3 and STAT3 factors dysregulated in circulating monocytes as well as in infarct macrophages in a mouse model of AMI (Figure IV in the online-only Data Supplement).

CD14^{+}HLA-DR$^{neg/low}$ monocytes did not suppress T-cell proliferation (Figure 2C), suggesting that the expanded population of monocytic cells in infarct patients are not immunosuppressive. Remarkably, macrophages differentiated from CD14^{+}HLA-DR$^{neg/low}$ monocytes by 4-day culture with M-CSF produced more TNFα, IL-6, and IL-1ß upon stimulation with IFNγ, as compared to macrophages generated from monocytes CD14^{+}HLA-DR^{high} (Figure 2D through 2F). These results indicate a crucial role for CD14^{+}HLA-DR$^{neg/low}$ monocytes in the complex immune response during AMI.

Normal-density CD10^{neg} neutrophils expand in the peripheral blood from patients with acute MI.

Neutrophil populations were analyzed in whole blood. CD16^{+}CD66b^{+}CD10^{neg} neutrophils were significantly increased in STEMI patients (Figure 3A, 3B and Table 2). Similarly to CD14^{+}HLA-DR$^{neg/low}$ monocytes ROC curve analysis of CD10^{neg} neutrophil frequencies, discriminating STEMI and UA patients revealed an AUC of 0.736 (95% CI: 0.601-0.871; P<0.01) but a lower AUC discriminating NSTEMI and UA patients (AUC=0.630; 95% CI: 0.414-0.847; P=0.054). By combining CD10^{neg} neutrophils with CK_{max} or LVEF AUC was increased to 0.885; (95% CI: 0.790-0980) and to 0.799 (95% CI: 0.636-0.961) respectively discriminating STEMI and UA patients (Figure 3C).

In patients with ACS the frequency of CD10^{neg} neutrophils significantly correlated with LVEF and CK_{max} (Figure 3D), as well as circulating levels of G-CSF (Figure IIIB in the online-only Data Supplement). AMI patients with higher systemic concentrations of G-CSF have increased CD10^{neg} neutrophils levels, suggesting G-CSF-driven neutrophil expansion. Noticeable, CD10^{neg} neutrophils, which expand proportional to the degree of myocardial injury/dysfunction, also significantly correlated with circulating levels of MMP-9, S100A9/S100A8, NGAL, MPO, IL-6, and IL-1ß (Figure IIIA in the online-only Data Supplement).

CD16^{+}CD66b^{+}CD10^{neg} neutrophils co-purified with the erythrocyte fraction following density gradient centrifugation. Low-density neutrophils were not present in mononuclear cell fraction obtained from AMI patients. Cytospin slides were made after FACS-sorting to

examine nuclear morphology (Figure 4A). We found that the majority of the $CD16^{+}CD66b^{+}CD10^{neg}$ cells has an immature morphology with a lobular nucleus, while $CD16^{+}CD66b^{+}CD10^{pos}$ cells are mature neutrophils with segmented nuclei (Figure 4A). These findings were obtained when neutrophils were isolated by dextran sedimentation as well as by negative selection using magnetic beads, indicating that the differences between the neutrophil subpopulations cannot be considered an artifact due to the isolation technique used.[8] $CD10^{neg}$ neutrophils sorted from blood of AMI patients express higher amounts of MMP-9 and S100A9 than $CD10^{pos}$ neutrophils (Figure 4B). The significant positive correlation between the frequency of $CD10^{neg}$ neutrophils and MMP-9/S100A9 serum levels suggests a mechanistic interdependence. No difference was found in the expression of ILR1, ILR2, MMP-8, NOS2, OLFM4 and STAT3, genes regulated in circulating neutrophils as well as in infarct neutrophils in a mouse model of AMI (Figure IV in the online-only Data Supplement).

A crucial role for neutrophils in the orchestration of adaptive immunity is emerging.[9-10] In an effort to define the immunoregulatory properties of $CD10^{neg}$ neutrophils we found that IFNγ production by $CD4^{+}$ T-cells was increased when co-cultured with $CD10^{neg}$ neutrophils using a transwell system (Figure 4C). Thus, normal-density $CD10^{neg}$ neutrophils from MI patients may modulate $CD4^{+}$ T-cell immune response in a cell contact-independent manner through soluble factors. Further studies aiming at deciphering the underlying mechanisms are mandatory.

Elevated circulating levels of IFNγ in cytomegalovirus-seropositive patients with expanded $CD10^{neg}$ neutrophils and increased frequency of $CD4^{+}CD28^{null}$ T-cells.

In a subgroup of patients we also performed flow cytometric immunophenotyping of lymphocyte subsets and investigated circulating levels of IFNγ (Figure 5 and Table in the online-only Data Supplement*)*. Patients with ACS were stratified in 4 subgroups based on frequency of $CD10^{neg}$ neutrophils (≤10% or >10%) and frequency of $CD4^{+}CD28^{null}$ T-cells (≤ 0.5% or >0.5%). Principal component analysis showed clustering according to elevated circulating levels of IFNγ, high levels of $CD10^{neg}$ neutrophils and peripheral expansion of $CD4^{+}CD28^{null}$ T-cells. The highest levels IFNγ were found in STEMI patients with expanded $CD10^{neg}$ neutrophils (> 10%) and increased frequency of $CD4^{+}CD28^{null}$ T-cells (Figure 5A and 5B). Across all patients with ACS an increased frequency of $CD4^{+}CD28^{null}$ T-cells was observed in CMV-seropositive individuals (Figure 5D), indicating that the expansion of $CD4^{+}CD28^{null}$ T-cells may not be a direct result of coronary events. Increased frequencies of

$CD28^{null}$ T-cells have been linked to cytomegalovirus (CMV) seropositivity.[11] Strikingly, when stratified according to CMV serostatus, the highest circulating levels of IFNγ were detected in CMV-seropositive STEMI patients displaying increased levels of $CD10^{neg}$ neutrophils (Figure 5D). Altogether, these findings suggest that $CD10^{neg}$ neutrophils may play an important role in determining the type of T helper cell response, especially in cytomegalovirus-seropositive patients with expanded peripheral $CD4^{+}CD28^{null}$ T cells.

Immature $CD101^{neg}$ neutrophils are rapidly recruited to sites of cardiac injury during ischemia/reperfusion.

Using next-generation RNA sequencing, we identified CD101 among the genes down-regulated by ischemia/reperfusion in circulating neutrophils (Figure IVB in the online-only Data Supplement) in a mouse model of AMI**.** Accordingly, we used CD101 as a cell surface marker to distinguishes immature from mature neutrophils among the heterogeneous $Ly6G^{pos}CXCR2^{pos}$ neutrophil populations, released into the bloodstream 90 minutes after reperfusion (Figure 6A). Circulating $CD11b^{bright}CD101^{pos}$ neutrophils have a normal-shaped nucleus, whereas immature neutrophils with a banded-shaped nucleus are $CD11b^{dim}CD101^{neg}$ (Figure 6B). A recent study in mice showed that banded neutrophils can be distinguished from mature neutrophils through CD101 expression and are associated with tumor progression.[12]

We then asked whether $CD101^{neg}$ neutrophils are recruited to site of ischemic injury after reperfusion. Flow cytometry analysis of immune cells isolated from the ischemic region 3 hours after reperfusion revealed infiltration of $CD11b^{pos}Ly6G^{pos}CD101^{neg}$ neutrophils, displaying increased expression of the matrix-degrading protease MMP-9 (Figure 6C). Moreover, we found that 24 hours after reperfusion $CD11b^{pos}Ly6G^{pos}CD101^{neg}$ neutrophils expressed IL-1ß at higher levels compared to $CD11b^{pos}Ly6G^{pos}CD101^{pos}$ cells (Figure 6D). These findings suggest that immature neutrophils may play an important role in the ischemic reperfused myocardium.

DISCUSSION

This study uncovered that CD10 can be used as a surface marker to identify the banded neutrophil subset that expands and drives proinflammatory effects in patients with AMI. We believe $CD10^{neg}$ neutrophils to derive from MI-induced altered myelopoiesis. Both mature and immature neutrophils are released presumably to meet the high demand for more neutrophils, especially in patients with large MI. Increased systemic levels of G-CSF, the primary regulator of emergency granulopoiesis,[9-10] are likely to drive the production/release of proinflammatory neutrophils from the bone marrow into the circulation. Accordingly, G-CSF-mediated immature $CD10^{neg}$ neutrophil expansion may be an adverse consequence of treating AMI patients with G-CSF. However, neutrophils may be released from the bone marrow in response to increased damage-associated molecular patterns such as S100A8/S100A9, secreted from necrotic/necroptotic cells and neutrophils as mediators of sterile inflammation.[13] We found that circulating $CD10^{neg}$ neutrophils express high amounts of S100A9, indicating banded neutrophils as a major source for this alarmin during AMI.

Under inflammatory conditions neutrophils traffic to inflamed tissues as well as to draining lymph nodes[9, 14] modulating T cell-mediated immune responses. Recently, CD10 has been proposed as a marker that distinguishes mature from immature neutrophils in healthy volunteers receiving G-CSF for stem cell mobilization.[15] Immunostimulatory $CD10^{neg}$ neutrophils and immunosuppressive $CD10^{pos}$ appear in the circulation of G-CSF–treated donors. However, human neutrophils can mimic myeloid-derived suppressor cells and suppress T-cell proliferation through artefactual mechanisms.[16] Of note, by performing transwell experiments we found that IFNγ production by $CD4^+$ T-cells was increased in the presence of $CD10^{neg}$ neutrophils. In systemic lupus erythematosus immature granulocytes have been shown to display a proinflammatory phenotype and to induce the production of IFNγ from $CD4^+$ T-cells by a contact-independent mechanism.[17]

Several cellular and molecular mechanisms may lead to increased circulating levels of IFNγ after AMI. Our principal component analysis showed clustering according to elevated circulating levels of IFNγ, high levels of $CD10^{neg}$ neutrophils and peripheral expansion of $CD4^+CD28^{null}$ T-cells. The function/role of $CD4^+CD28^{null}$ T-cells in coronary artery disease and atherogenesis is far from clear. $CD4^+CD28^{null}$ T-cells are long-lived cytotoxic T helper cells, secreting high levels of IFNγ.[18] A recent study revealed complex associations between of $CD4^+CD28^{null}$ T-cells and cardiovascular disease.[19] $CD4^+CD28^{null}$ T cells are associated with a lower risk for first-time coronary events in a population-based cohort. In contrast, in patients with advanced atherosclerotic disease an increased frequency of $CD4^+CD28^{null}$ T-cells was

associated with more frequent major adverse cardiovascular events.[19] Noteworthy, in our study the expansion of $CD4^{+}CD28^{null}$ T-cells was closely linked to CMV infection across all patients with ACS. CMV has been associated with atherosclerosis and increased risk for cardiovascular diseases. Recent clinical data showed that myocardial ischemia in CMV-seropositive patients leads to significant changes in the composition of the $CD8^{+}$ T-cell repertoire, accelerating immunosenescence.[20] Overall, our findings point to a potential link among increased frequency of normal-density $CD10^{neg}$ neutrophils, circulating $CD4^{+}CD28^{null}$ T-cells and elevated IFNγ levels, especially in cytomegalovirus-seropositive patients. Thus, determination of circulating $CD10^{neg}$ neutrophils levels, particularly in the context of CMV infection, might help to identify patients at risk for excessive inflammatory immune response.

In spite of numerous studies on polymorphonuclear myeloid cells the role of immature neutrophils is underexplored in the setting of AMI in mice. We found that CD101 can be used as a surface marker to identify the banded neutrophil subset among the heterogeneous $CD11b^{pos}Ly6G^{pos}$ neutrophil populations in blood and infarct tissues during ischemia/reperfusion. Previous studies in a human model of experimental endotoxemia showed that banded neutrophils exhibit efficient migration to sites of infection.[21] Moreover, developmental analysis of bone marrow neutrophils revealed that immature neutrophils are recruited to the periphery of tumor-bearing mice.[12] Of note, we found that $CD101^{neg}$ neutrophils are released into the bloodstream within minutes after reperfusion and are capable of efficient migration to ischemic tissues, displaying increased expression of MMP-9 and IL-1ß at 3 and 24 hours after reperfusion, respectively. There are significant differences between mouse and human immunology[22] and the transit time of leukocytes may be quite different.[23] During homeostasis, trafficking of neutrophils/myeloid cells from bone marrow into the circulation takes between 1–2 days in mice and 5-8 days in humans.[23] Such differences should be considered when comparing animal and human studies on immune mechanisms underlying wound healing.

The recruitment of immune cells to sites of tissue repair is a complex process involving cytokines, chemokines, and interactions between infiltrating immune cells. $CD14^{+}HLA\text{-}DR^{neg/low}$ monocytes from patients with AMI are not immunosuppressive but express high amounts of IL1R1. Thus, immature neutrophils, as an important source of IL1ß in the reperfused heart, may be actively involved in the recruitment of $CD14^{+}HLA\text{-}DR^{neg/low}$ monocytes. Saxena *et al.*[24] showed that IL1R1 signaling mediates early recruitment of $Ly6C^{hi}$ monocytes to the infarcted myocardium. Reperfused myocardial infarction had intense infiltration with $Ly6C^{hi}$

monocytes expressing IL1R1 that peaked after 24 hours of reperfusion.[24] Noteworthy, recent studies demonstrated that the failing human heart also contains HLA-DR$^{neg/low}$ monocytes.[7]

Several immune mechanisms operate during cardiac wound healing and IFNγ plays different roles depending on the cellular and microenvironmental context intrinsically linked to the stages of ischemic injury. By integrating cell sorting and *in vitro* experiments we found that macrophages differentiated from CD14^{+}HLA-DR$^{neg/low}$ monocytes produced more TNFα, IL-6, and IL-1ß upon IFNγ stimulation as CD14^{+}HLA-DR^{high} monocyte-derived macrophages. These findings may support a role for CD14^{+}HLA-DR$^{neg/low}$ cells in pathogenic mechanisms operating during AMI and may, at least in part, explain why increased immature monocytic cells frequency correlate with circulating levels of TNFα, IL-6, and IL-1ß.

The interleukin-1 pathway has been shown to play a key pathogenetic role in post-MI inflammation and the progression to heart failure.[25] Our *in vitro* mechanistic experiments with neutrophils/monocytes from patients with AMI as well as mouse studies provide a potential linkage between the induction of immature myeloid cells and increased interleukin-1 activity during AMI. Emerging evidences highlight that targeting interleukin-1 may hold promise for patients after MI.[26] In STEMI patients the interleukin-1 receptor antagonist anakinra significantly reduced the systemic inflammatory response. Moreover, in the CANTOS trial, administration of canakinumab (a monoclonal antibody targeting IL1β) prevented the recurrence of ischemic events, reduced heart failure-related hospitalizations and mortality in patients with prior AMI.[26]

In summary, we demonstrate that CD14^{+}HLA-DR$^{lo/neg}$ monocytes and normal-density CD10^{neg} neutrophils driving proinflammatory responses expand in patients with AMI. These findings could have major implications for understanding immunoregulatory mechanisms operating during AMI and for the development of future therapeutic strategies. Nevertheless, further studies deciphering the relationship between elevated immature granulocytic and monocytic cells and ensuing mortality and morbidity after ischemic injury are necessary and ongoing.

Acknowledgments

We are grateful for the support of Dr Matthias Ballmaier from the Central Research Facility Cell Sorting of the Hannover Medical School.

Sources of Funding

D. Fraccarollo and J. Bauersachs received support from the Deutsche Forschungsgemeinschaft (BA 1742/8-1).

Disclosures

None.

References

1. Heusch G, Gersh B. The pathophysiology of acute myocardial infarction and strategies of protection beyond reperfusion: a continual challenge. *Eur Heart J* 2017;38:774-784.
2. Gabrilovich D, Nagaraj S. Myeloid-derived suppressor cells as regulators of the immune system. *Nat Rev Immunol* 2009;9:162-174.
3. Silvin A, Chapuis N, Dunsmore G, Goubet A-G, Dubuisson A, Derosa L, Almire C, Hénon C, Kosmider O, Droin N, Rameau P, Catelain C, Alfaro A, Dussiau C, Friedrich C, Sourdeau E, Marin N, Szwebel T-A, Cantin D, Mouthon L, Borderie D, Deloger M, Bredel D, Mouraud S, Drubay D, Andrieu M, Lhonneur A-S, Saada V, Stoclin A, Willekens C, Pommeret F, Griscelli F, Ng LG, Zhang Z, Bost P, Amit I, Barlesi F, Marabelle A, Pène F, Gachot B, André F, Zitvogel L, Ginhoux F, Fontenay M, Solary E. Elevated Calprotectin and Abnormal Myeloid Cell Subsets Discriminate Severe from Mild COVID-19. *Cell* 2020;182:1401-1418.
4. Schulte-Schrepping J, Reusch N, Paclik D, Bassler K, Schlickeiser S, Zhang B, Kramer B, Krammer T, Brumhard S, Bonaguro L, De Domenico E, Wendisch D, Grasshoff M, Kapellos TS, Beckstette M, Pecht T, Saglam A, Dietrich O, Mei HE, Schulz AR, Conrad C, Kunkel D, Vafadarnejad E, Xu CJ, Horne A, Herbert M, Drews A, Thibeault C, Pfeiffer M, Hippenstiel S, Hocke A, Muller-Redetzky H, Heim KM, Machleidt F, Uhrig A, Bosquillon de Jarcy L, Jurgens L, Stegemann M, Glosenkamp CR, Volk HD, Goffinet C, Landthaler M, Wyler E, Georg P, Schneider M, Dang-Heine C, Neuwinger N, Kappert K, Tauber R, Corman V, Raabe J, Kaiser KM, Vinh MT, Rieke G, Meisel C, Ulas T, Becker M, Geffers R, Witzenrath M, Drosten C, Suttorp N, von Kalle C, Kurth F,

Handler K, Schultze JL, Aschenbrenner AC, Li Y, Nattermann J, Sawitzki B, Saliba AE, Sander LE. Severe COVID-19 Is Marked by a Dysregulated Myeloid Cell Compartment. *Cell* 2020;182:1419-1440.

5. Haghikia A, Li XS, Liman TG, Bledau N, Schmidt D, Zimmermann F, Krankel N, Widera C, Sonnenschein K, Weissenborn K, Fraccarollo D, Heimesaat MM, Bauersachs J, Wang Z, Zhu W, Bavendiek U, Hazen SL, Endres M, Landmesser U. Gut Microbiota-Dependent Trimethylamine N-Oxide Predicts Risk of Cardiovascular Events in Patients With Stroke and Is Related to Proinflammatory Monocytes. *Arterioscler Thromb Vasc Biol* 2018;38:2225-2235.
6. Murray PJ, Allen JE, Biswas SK, Fisher EA, Gilroy DW, Goerdt S, Gordon S, Hamilton JA, Ivashkiv LB, Lawrence T, Locati M, Mantovani A, Martinez FO, Mege JL, Mosser DM, Natoli G, Saeij JP, Schultze JL, Shirey KA, Sica A, Suttles J, Udalova I, van Ginderachter JA, Vogel SN, Wynn TA. Macrophage activation and polarization: nomenclature and experimental guidelines. *Immunity* 2014;41:14-20.
7. Bajpai G, Schneider C, Wong N, Bredemeyer A, Hulsmans M, Nahrendorf M, Epelman S, Kreisel D, Liu Y, Itoh A, Shankar T, Selzman C, Drakos S, Lavine K. The human heart contains distinct macrophage subsets with divergent origins and functions. *Nat Med* 2018;24:1234-1245.
8. Hardisty G, LLanwarne F, Minns D, Gillan J, Davidson D, Findlay E, Gray R. Ultra-pure isolation of low density neutrophils casts doubt on their exceptionality in health and disease. *bioRxiv* 2020:2020.06.17.156588.
9. Costa S, Bevilacqua D, Cassatella MA, Scapini P. Recent advances on the crosstalk between neutrophils and B or T lymphocytes. *Immunology* 2019;156:23-32.
10. Silvestre-Roig C, Braster Q, Ortega-Gomez A, Soehnlein O. Neutrophils as regulators of cardiovascular inflammation. *Nat Rev Cardiol* 2020;17:327-340.
11. Pera A, Caserta S, Albanese F, Blowers P, Morrow G, Terrazzini N, Smith HE, Rajkumar C, Reus B, Msonda JR, Verboom M, Hallensleben M, Blasczyk R, Davies KA, Kern F. CD28(null) pro-atherogenic CD4 T-cells explain the link between CMV infection and an increased risk of cardiovascular death. *Theranostics* 2018;8:4509-4519.
12. Evrard M, Kwok IWH, Chong SZ, Teng KWW, Becht E, Chen J, Sieow JL, Penny HL, Ching GC, Devi S, Adrover JM, Li JLY, Liong KH, Tan L, Poon Z, Foo S, Chua JW, Su IH, Balabanian K, Bachelerie F, Biswas SK, Larbi A, Hwang WYK, Madan V, Koeffler HP, Wong SC, Newell EW, Hidalgo A, Ginhoux F, Ng LG. Developmental Analysis of

Bone Marrow Neutrophils Reveals Populations Specialized in Expansion, Trafficking, and Effector Functions. *Immunity* 2018;48:364-379.

13. Sreejit G, Abdel-Latif A, Athmanathan B, Annabathula R, Dhyani A, Noothi SK, Quaife-Ryan GA, Al-Sharea A, Pernes G, Dragoljevic D, Lal H, Schroder K, Hanaoka BY, Raman C, Grant MB, Hudson JE, Smyth SS, Porrello ER, Murphy AJ, Nagareddy PR. Neutrophil-Derived S100A8/A9 Amplify Granulopoiesis After Myocardial Infarction. *Circulation* 2020;141:1080-1094.
14. Leliefeld PH, Koenderman L, Pillay J. How Neutrophils Shape Adaptive Immune Responses. *Front Immunol* 2015;6:471.
15. Marini O, Costa S, Bevilacqua D, Calzetti F, Tamassia N, Spina C, De Sabata D, Tinazzi E, Lunardi C, Scupoli MT, Cavallini C, Zoratti E, Tinazzi I, Marchetta A, Vassanelli A, Cantini M, Gandini G, Ruzzenente A, Guglielmi A, Missale F, Vermi W, Tecchio C, Cassatella MA, Scapini P. Mature CD10(+) and immature CD10(-) neutrophils present in G-CSF-treated donors display opposite effects on T cells. *Blood* 2017;129:1343-1356.
16. Negorev D, Beier UH, Zhang T, Quatromoni JG, Bhojnagarwala P, Albelda SM, Singhal S, Eruslanov E, Lohoff FW, Levine MH, Diamond JM, Christie JD, Hancock WW, Akimova T. Human neutrophils can mimic myeloid-derived suppressor cells (PMN-MDSC) and suppress microbead or lectin-induced T cell proliferation through artefactual mechanisms. *Sci Rep* 2018;8:3135.
17. Rahman S, Sagar D, Hanna RN, Lightfoot YL, Mistry P, Smith CK, Manna Z, Hasni S, Siegel RM, Sanjuan MA, Kolbeck R, Kaplan MJ, Casey KA. Low-density granulocytes activate T cells and demonstrate a non-suppressive role in systemic lupus erythematosus. *Ann Rheum Dis* 2019;78:957-966.
18. Dumitriu IE, Araguás ET, Baboonian C, Kaski JC. CD4+CD28null T cells in coronary artery disease: when helpers become killers. *Cardiovasc Res* 2008;81:11-19.
19. Tomas L, Bengtsson E, Andersson L, Badn W, Tengryd C, Persson A, Edsfeldt A, Nilsson P, Schiopu A, Nilsson J, Gonçalves I, Björkbacka H. Low Levels of CD4+CD28null T Cells at Baseline Are Associated With First-Time Coronary Events in a Prospective Population-Based Case-Control Cohort. *Arterioscler Thromb Vasc Biol* 2020;40:426-436.
20. Hoffmann J, Shmeleva EV, Boag SE, Fiser K, Bagnall A, Murali S, Dimmick I, Pircher H, Martin-Ruiz C, Egred M, Keavney B, Zglinicki Tv, Das R, Todryk S, Spyridopoulos I. Myocardial Ischemia and Reperfusion Leads to Transient CD8 Immune Deficiency and Accelerated Immunosenescence in CMV-Seropositive Patients. *Circ Res* 2015;116:87-98.

21. van Grinsven E, Textor J, Hustin LSP, Wolf K, Koenderman L, Vrisekoop N. Immature Neutrophils Released in Acute Inflammation Exhibit Efficient Migration despite Incomplete Segmentation of the Nucleus. *J Immunol* 2019;202:207-217.
22. Javier M, Hughes H. Of Mice and Not Men: Differences between Mouse and Human Immunology. *J Immunol* 2004;172:2731-2738.
23. Mackey JBG, Coffelt SB, Carlin LM. Neutrophil Maturity in Cancer. *Front Immunol* 2019;10.1912.
24. Saxena A, Chen W, Su Y, Rai V, Uche OU, Li N, Frangogiannis NG. IL-1 Induces Proinflammatory Leukocyte Infiltration and Regulates Fibroblast Phenotype in the Infarcted Myocardium. *J Immunol* 2013;191:4838-4848.
25. Abbate A, Toldo S, Marchetti C, Kron J, Tassell BWV, Dinarello CA. Interleukin-1 and the Inflammasome as Therapeutic Targets in Cardiovascular Disease. *Circ Res* 2020;126:1260-1280.
26. Buckley LF, Abbate A. Interleukin-1 blockade in cardiovascular diseases: a clinical update. *Eur Heart J* 2018;39:2063-2069.

Figure Legends

Figure 1. Increased circulating levels of CD14^{+}HLA-DR$^{neg/low}$ monocytes in patients with AMI. (A) Gating strategy to identify CD14^{+}HLA-DR$^{neg/low}$ monocytes. (B) Frequency of CD14^{+}HLA-DR$^{neg/low}$ monocytes in healthy control subjects (CTR, n=17) and in patients with unstable angina (UA; n=11), non-ST-elevation MI (NSTEMI, n=16), and ST-elevation MI (STEMI, n=44). (C) Receiver operator characteristic (ROC) curve of CD14^{+}HLA-DR$^{neg/low}$ monocytes discriminating STEMI/NSTEMI and UA patients and the combination of CD14^{+}HLA-DR$^{neg/low}$ monocytes with LV ejection fraction (LVEF) or maximum CK (CK_{max}). (D) Linear regression analysis between the frequency of CD14^{+}HLA-DR$^{neg/low}$ monocytes, LVEF and CK_{max} in patients with acute coronary syndrome. *P<0.05, STEMI vs. UA.

Figure 2. CD14^{+}HLA-DR$^{neg/low}$ monocytes from patients with AMI are not immunosuppressive but exhibit an inflammatory phenotype. (A) May-Grünwald Giemsa stained cytospin preparations of CD14^{+}HLA-DR$^{neg/low}$ and CD14^{+}HLA-DR^{high} monocytes (B) Relative RNA expression of S100A9 and IL1R1 in CD14^{+}HLA-DR$^{neg/low}$ versus CD14^{+}HLA-DR^{high} monocytes. (C) T-cell activation by anti CD3/CD28 beads in presence/absence of CD14^{+}HLA-DR$^{neg/low}$ or CD14^{+}HLA-DR^{high} monocytes assessed by CellTrace™ Violet dilution after 96 hours of co-culture. (D) Macrophages differentiated from CD14^{+}HLA-DR$^{neg/low}$ monocytes and (E) CD14^{+}HLA-DR^{high} cells by 4-day culture with M-CSF. (F) TNFα, IL-6, and IL-1ß in supernatants of macrophage cultures upon stimulation with IFNγ.

M^{b}=baseline. CD14^{+}HLA-DR$^{neg/low}$/CD14^{+}HLA-DR^{high} cells were isolated by flow-cytometric sorting from patients with AMI (n=5-6). *P<0.05.

Figure 3. Circulating normal-density CD10^{neg} neutrophils increase in patients with AMI. (A) Gating strategy to identify CD10^{neg} neutrophils (B) Frequency of CD16^{+}CD66b^{+}CD10^{neg} neutrophils in healthy control subjects (CTR, n=17) and in patients with unstable angina (UA; n=11), non-ST-elevation MI (NSTEMI, n=16), and ST-elevation MI (STEMI, n=44). (C) Receiver operator characteristic (ROC) curve of CD10^{neg} neutrophils discriminating STEMI/NSTEMI and UA patients and the combination of CD10^{neg} neutrophils with LV ejection fraction (LVEF) or maximum CK (CK_{max}). (D) Linear regression analysis between the frequency of CD10^{neg} neutrophils, LVEF and CK_{max} in patients with acute coronary syndrome. *P<0.05; STEMI vs. UA.

Figure 4. CD10^{neg} neutrophils from patients with AMI express high amounts of MMP-9 and S100A9 and increase IFNγ production by CD4^{+} T-cells. (A) May-Grünwald Giemsa stained cytospin preparations of CD16^{+}CD66b^{+}CD10^{neg} and CD16^{+}CD66b^{+}CD10^{pos} cells. (B) Relative RNA expression of MMP9 and S100A9 in CD10^{neg} versus CD10^{pos} neutrophils. (C) IFNγ production by CD4^{+}T cells stimulated with anti-CD3/CD28 beads and co-cultured for 48 hours in presence/absence of CD10^{neg} or CD10^{pos} neutrophils using a transwell system. CD10^{neg}/CD10^{pos} neutrophils were isolated by flow-cytometric sorting from patients with AMI (n=5). *P<0.05.

Figure 5. Elevated circulating IFNγ levels in cytomegalovirus-seropositive patients with expanded CD10^{neg} neutrophils and increased frequency of CD4^{+}CD28^{null} T-cells. (A) Principal component analysis showing clustering according to circulating levels of IFNγ, CD10^{neg} neutrophils and peripheral CD4^{+}CD28^{null} T-cells. (B) Scatter plot showing IFNγ levels according to frequency of CD10^{neg} neutrophils and CD4^{+}CD28^{null} T-cells. Patients with unstable angina (UA; n=11), non-ST-elevation MI (NSTEMI, n=13), and ST-elevation MI (STEMI, n=34) were stratified based on frequency of CD10^{neg} neutrophils (≤10% or >10%) and frequency of CD4^{+}CD28^{null} T-cells (≤0.5% or >0.5%). (C) Gating strategy to identify CD4^{+}CD28^{null} T-cells. (D) Frequency of CD4^{+}CD28^{null} T-cells and circulating IFNγ levels stratified according to cytomegalovirus (CMV) serostatus. *P<0.05.

Figure 6. Immature CD101^{neg} neutrophils are rapidly recruited to ischemic sites and are a major source of MMP-9 and IL-1ß in the reperfused myocardium in a mouse model of AMI. (A) Representative gating strategy to identify circulating immature neutrophils among CD11b^{pos}Ly6G^{pos}CXCR2^{pos} cells and number of CD11b^{dim}CD101^{neg} and CD11b^{bright}CD101^{pos} neutrophils released into the bloodstream 90 minutes after ischemia/reperfusion. (B) May-Grünwald Giemsa stained cytospin preparations of sorted CD11b^{dim}CD101^{neg} and CD11b^{bright}CD101^{pos} neutrophils. (C) Flow cytometric gating strategy to identify neutrophils in the ischemic region 3 hours after reperfusion and mean fluorescent intensity (MFI) of MMP-9 on CD101^{neg} and CD101^{pos} neutrophils. (D) Flow cytometry identifying infarct neutrophils 24 hours after ischemia/reperfusion and mean fluorescent intensity of IL-1ß on CD101^{neg} and CD101^{pos} neutrophils. n=3-4; *P<0.05.

Summarizing figure. $CD14^{+}HLA\text{-}DR^{neg/low}$ monocytes and normal-density $CD10^{neg}$ neutrophils inducing proinflammatory and adaptive immune responses emerge in patients with large acute myocardial infarction.

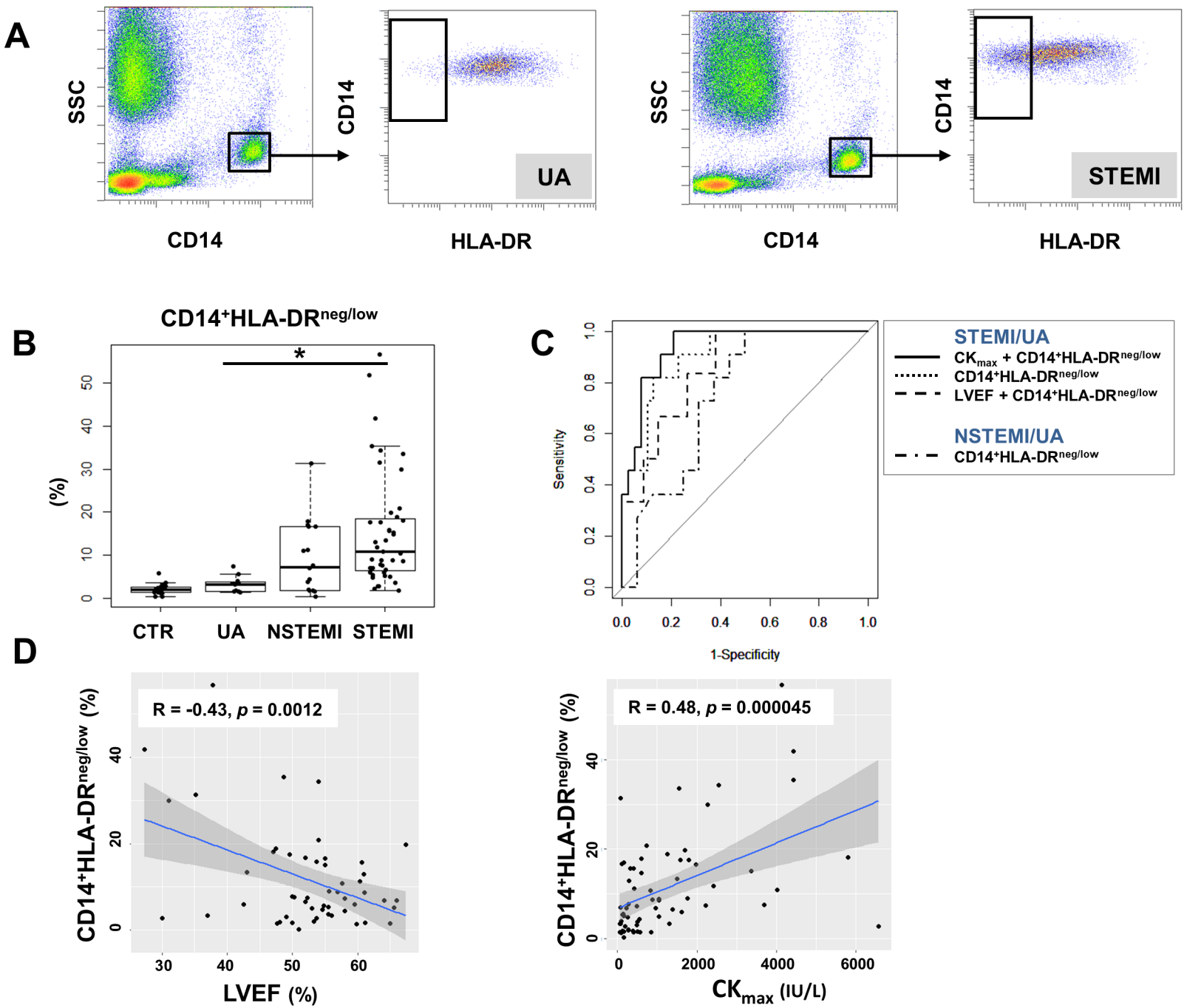
A
SSC
CD14
CD14
HLA-DR
UA
SSC
CD14
CD14
HLA-DR
STEMI
B
CD14+HLA-DRneg/low
*
(%)
CTR
UA
NSTEMI
STEMI
C
Sensitivity
1-Specificity
STEMI/UA
CKmax + CD14+HLA-DRneg/low
CD14+HLA-DRneg/low
LVEF + CD14+HLA-DRneg/low
NSTEMI/UA
CD14+HLA-DRneg/low
D
R = -0.43, p = 0.0012
CD14+HLA-DRneg/low (%)
LVEF (%)
R = 0.48, p = 0.000045
CD14+HLA-DRneg/low (%)
CKmax (IU/L)

Figure 1

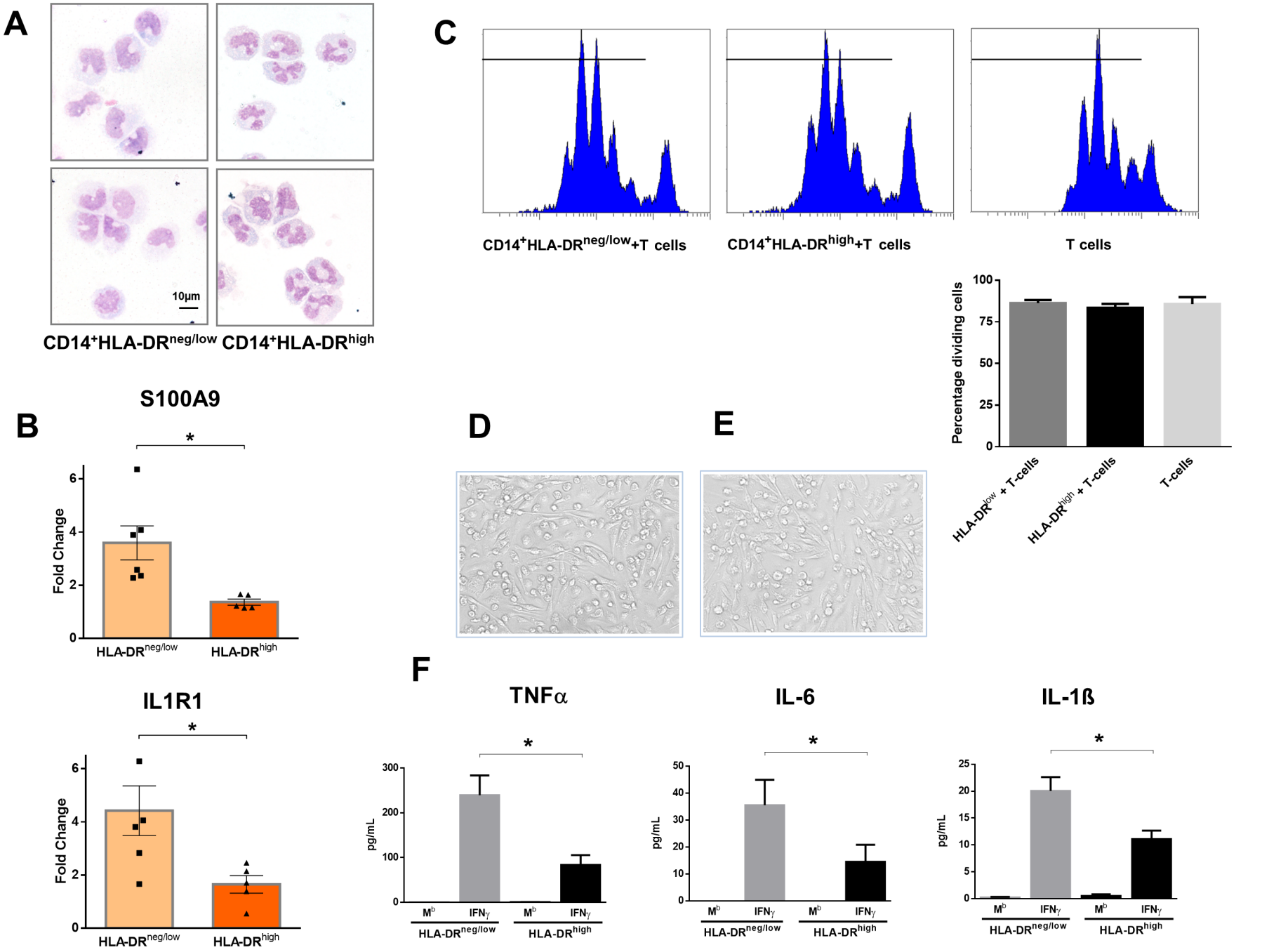
A
10µm
CD14+HLA-DRneg/low
CD14+HLA-DRhigh
C
CD14+HLA-DRneg/low+T cells
CD14+HLA-DRhigh+T cells
T cells
Percentage dividing cells
100
75
50
25
0
HLA-DRlow + T-cells
HLA-DRhigh + T-cells
T-cells
B
S100A9
*
Fold Change
6
4
2
0
HLA-DRneg/low
HLA-DRhigh
D
E
F
IL1R1
*
Fold Change
6
4
2
0
HLA-DRneg/low
HLA-DRhigh
TNFα
*
pg/mL
300
200
100
0
Mb
IFNγ
Mb
IFNγ
HLA-DRneg/low
HLA-DRhigh
IL-6
*
pg/mL
50
40
30
20
10
0
Mb
IFNγ
Mb
IFNγ
HLA-DRneg/low
HLA-DRhigh
IL-1ß
*
pg/mL
25
20
15
10
5
0
Mb
IFNγ
Mb
IFNγ
HLA-DRneg/low
HLA-DRhigh

Figure 2

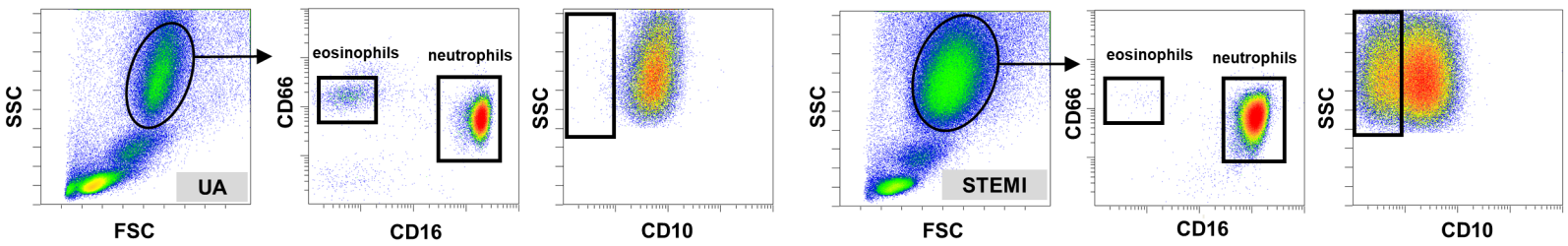
A
SSC
FSC
UA
CD66
CD16
eosinophils
neutrophils
SSC
CD10
SSC
FSC
STEMI
CD66
CD16
eosinophils
neutrophils
SSC
CD10

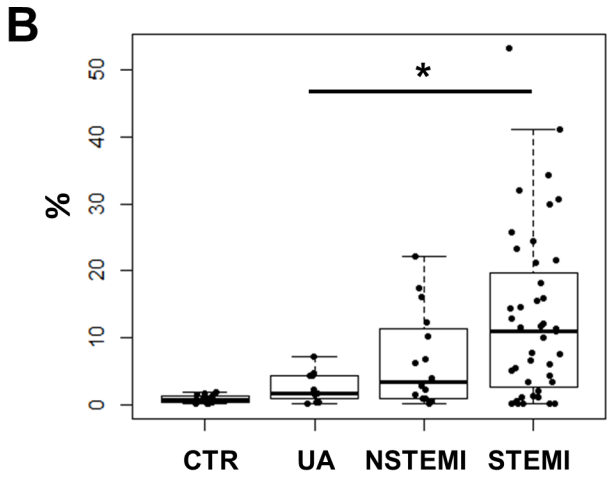
B
%
0
10
20
30
40
50
*
CTR
UA
NSTEMI
STEMI

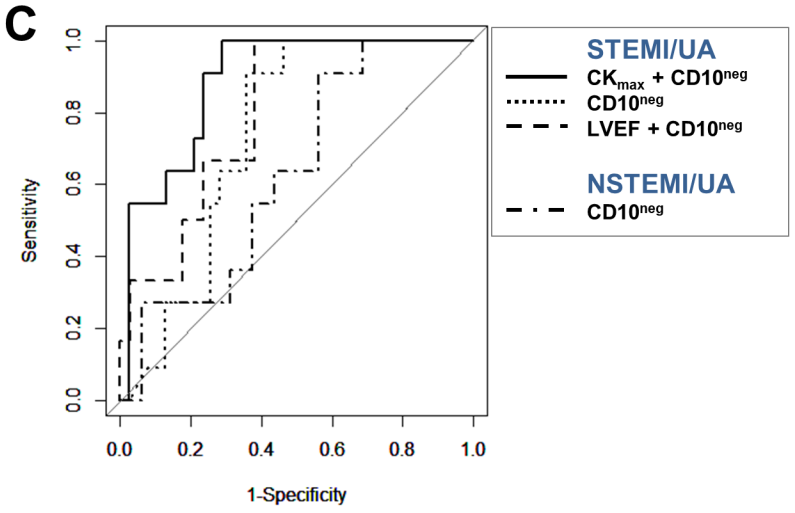
C
Sensitivity
1-Specificity
0.0
0.2
0.4
0.6
0.8
1.0
STEMI/UA
CKmax + CD10neg
CD10neg
LVEF + CD10neg
NSTEMI/UA
CD10neg

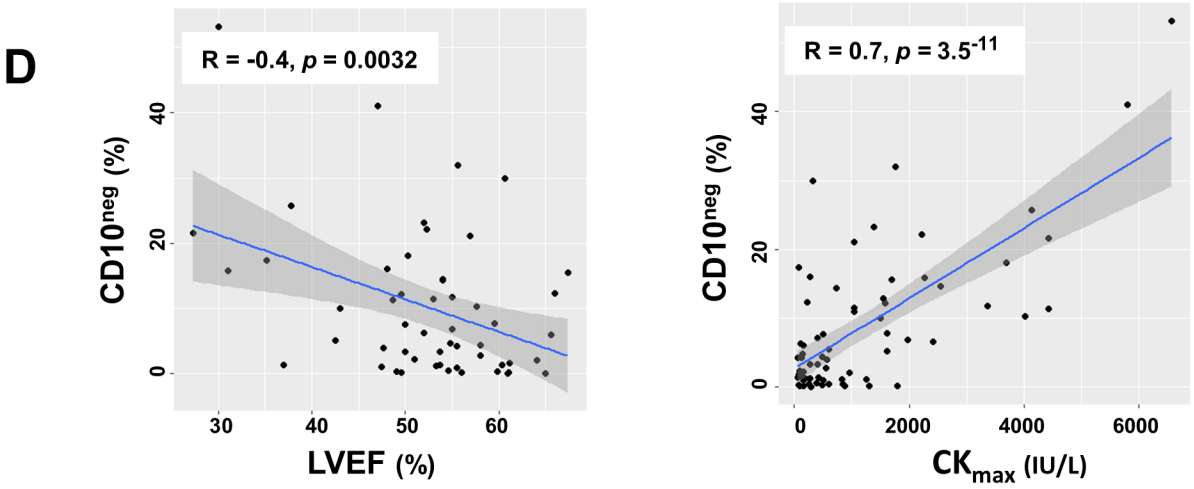
D
R = -0.4, p = 0.0032
CD10neg (%)
LVEF (%)
30
40
50
60
R = 0.7, p = 3.5-11
CD10neg (%)
CKmax (IU/L)
0
2000
4000
6000

Figure 3

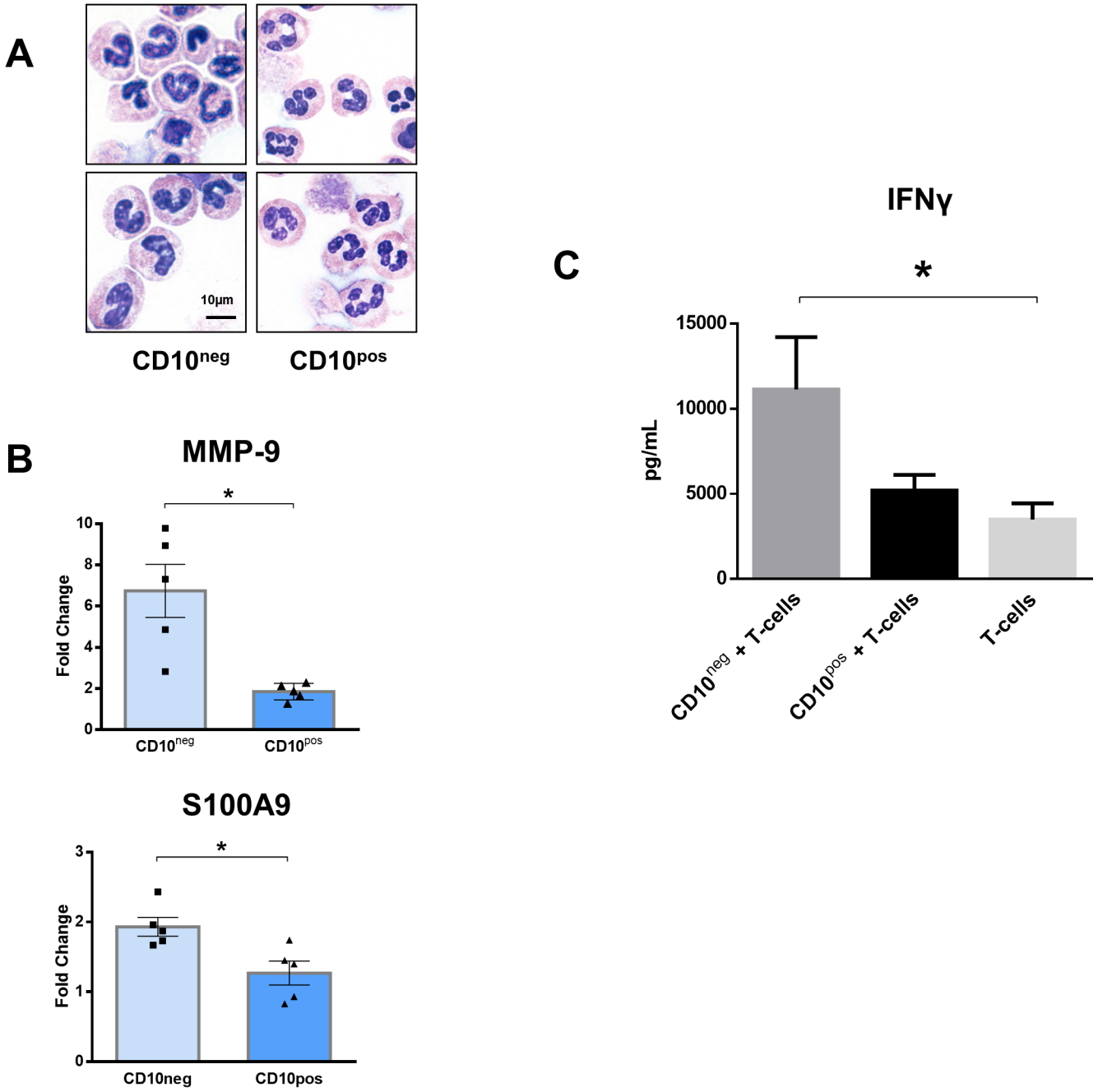
A
10µm
CD10neg
CD10pos
B
MMP-9
*
Fold Change
10
8
6
4
2
0
CD10neg
CD10pos
S100A9
*
Fold Change
3
2
1
0
CD10neg
CD10pos
C
IFNγ
*
pg/mL
15000
10000
5000
0
CD10neg + T-cells
CD10pos + T-cells
T-cells

Figure 4

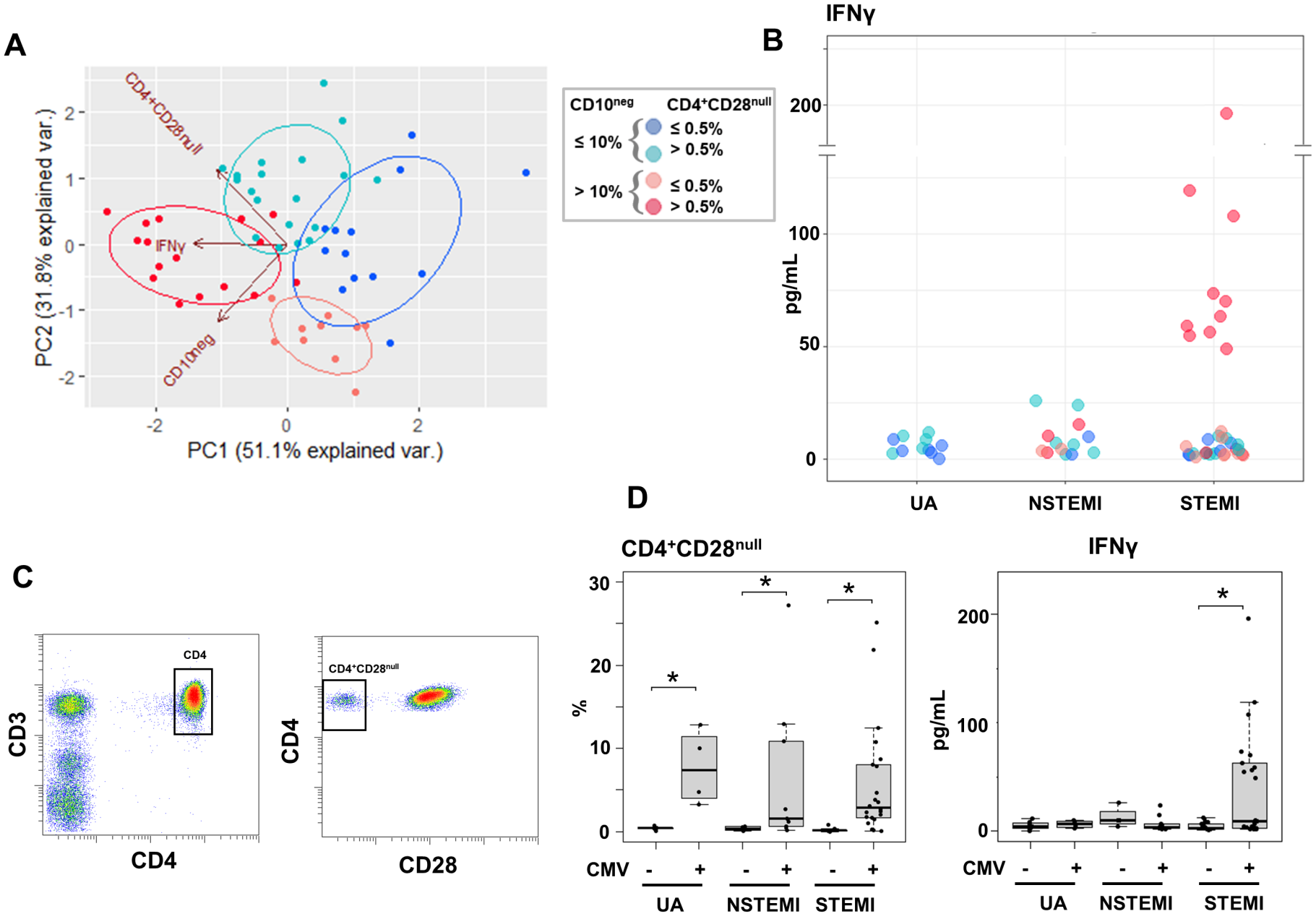
A
CD4+CD28null
IFNγ
CD10neg
PC2 (31.8% explained var.)
PC1 (51.1% explained var.)
CD10neg
CD4+CD28null
≤ 10%
≤ 0.5%
> 0.5%
> 10%
≤ 0.5%
> 0.5%
B
IFNγ
pg/mL
UA
NSTEMI
STEMI
C
CD4
CD3
CD4
CD4+CD28null
CD28
D
CD4+CD28null
%
CMV
UA
NSTEMI
STEMI
IFNγ
pg/mL
CMV
UA
NSTEMI
STEMI

Figure 5

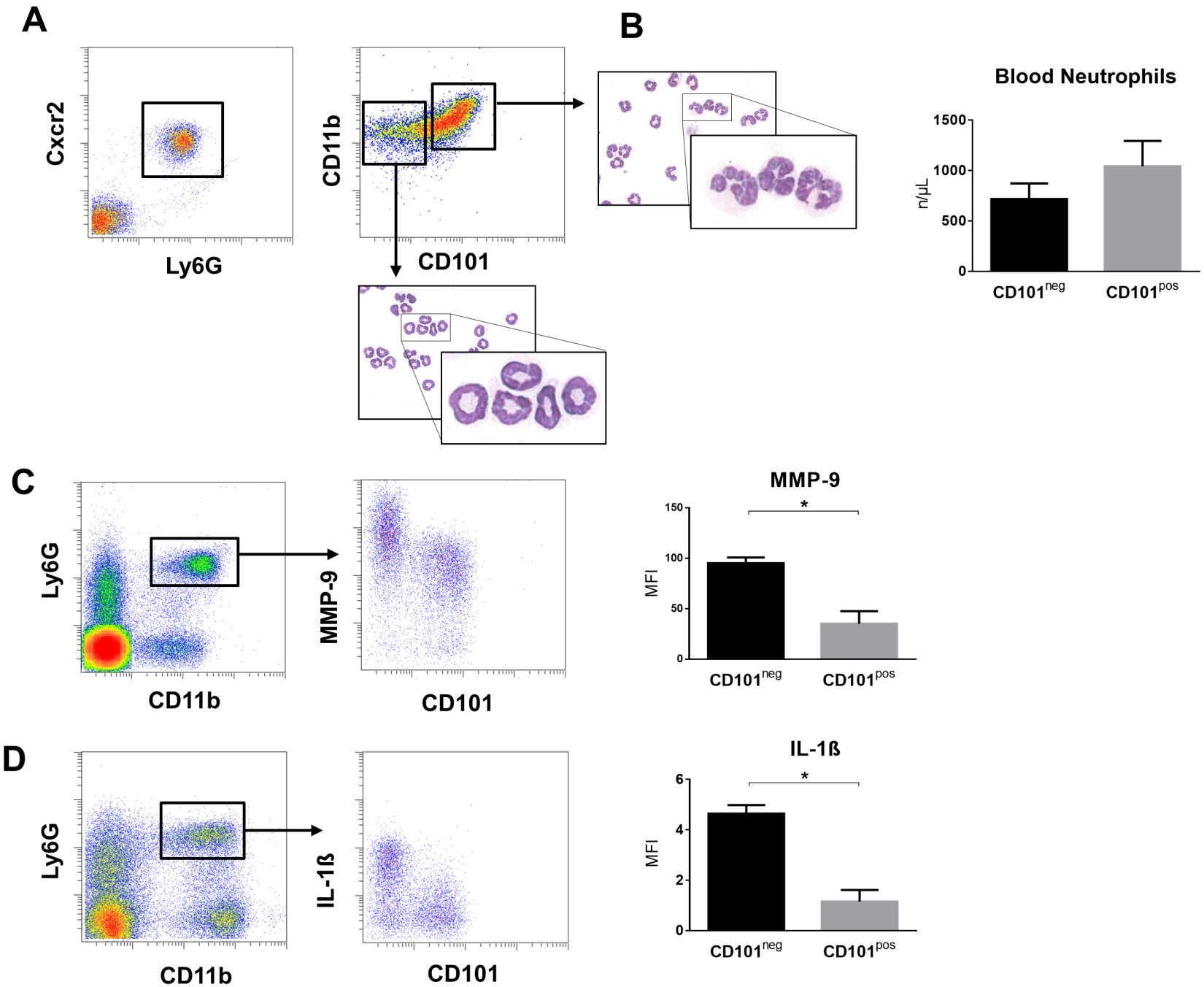
A
Cxcr2
Ly6G
CD11b
CD101
B
Blood Neutrophils
1500
1000
500
0
n/µL
CD101neg
CD101pos
C
Ly6G
CD11b
MMP-9
CD101
MMP-9
150
100
50
0
MFI
*
CD101neg
CD101pos
D
Ly6G
CD11b
IL-1ß
CD101
IL-1ß
6
4
2
0
MFI
*
CD101neg
CD101pos

Figure 6

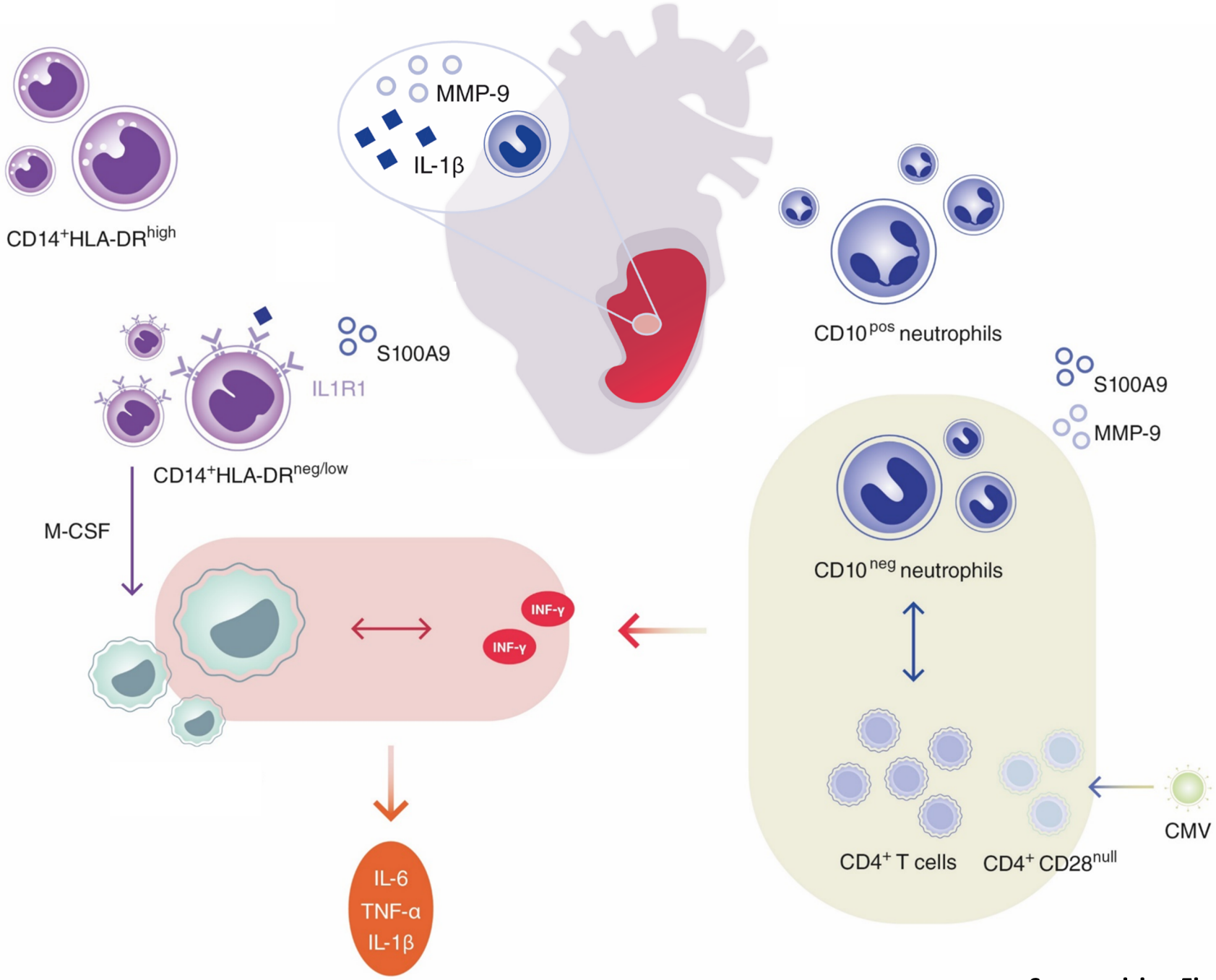

Summarizing Figure

Table 1. General Traits

		UA (*n*=11)	NSTEMI (*n*=16)	STEMI (*n*=44)
Age (years)		63.3±2.5	64.1±3.6	60.1±1.5
Gender	Male/Female	36/8	14/2	9/2
BMI (kg/m^2)		27.5±0.9	27.9±0.9	27.5±0.7
Blood analyses	LDL(mg/dL)	92.2±19.2	94.9±9.5	138.8±7.4
	CK (at admission) (IU/L)	202.0±54.4	216.4±36.2	609.9±108.2
	CK_{max} (IU/L)	202.6±54.2	748.4±270.2	1705.1±233.7
	CK-MB (IU/L)	19.1±1.2	37.7±6.5	72.3±10.1
	Troponin (ng/L)	15.0±3.4	267.6±110.3	825.8±218.7
	Creatinine (µmol/L)	83.0±4.5	90.9±4.8	97.6±8.3
	CRP (mg/L)	2.6±0.7	3.4±1.0	4.9±1.9

Data are presented as mean±SD. LDL, low density lipoprotein; CK, creatine kinase; CK_{max}, maximum CK; CK-MB, creatine kinase-myocardial band; CRP, C-reactive protein.

Table 2. Leukocyte Count and Monocyte/Neutrophil Subsets

	CTR (*n* = 17)	UA (*n*=11)	NSTEMI (*n*=16)	STEMI (*n*=44)	*p* (K-W)
Neutrophil (10^3/µL)	3.25 (2.74-3.42)	4.05 (3.64-4.56)*	5.72 (4.80-7.79)*†	6.13 (5.17-7.17)*†	<0.0001
Monocyte (10^3/µL)	0.64 (0.53-0.74)	0.74 (0.49-0.80)	0.87 (0.72-1.03)*†	0.99 (0.77-1.26)*†	<0.001
Lymphocyte (10^3/µL)	2.20 (1.96-2.47)	1.82 (1.55-1.98)	1.96 (1.76-2.49)	2.08 (1.62-2.67)	0.282
Lymphocyte/Neutrophil ratio	0.70 (0.57-0.79)	0.45 (0.38-0.55)*	0.32 (0.28-0.44)*	0.35 (0.28-0.45)*	<0.0001
Eosinophil (10^3/µL)	0.16 (0.10-0.30)	0.15 (0.11-0.16)	0.20(0.14-0.33)	0.12 (0.06-0.20)	0.100
Monocyte Classical (*n*/µL)	476 (334-583)	332 (243-388)	509 (454-719)†	522 (391-718)†	<0.05
Monocyte Intermediate (*n*/µL)	130 (73-145)	186 (131-366)*	203 (143-309)*	249 (164-399)*	<0.001
Monocyte Non Classical (*n*/µL)	48 (30-64)	50 (37-66)	64 (47-108)	99 (57-137)*†	<0.001
$CD10^{neg}$ (*n*/µL)	22(9-31)	66(30-178)*	197(50-714)*	635(130-1081)*†	<0.0001
$CD14^{+}HLA\text{-}DR^{neg/low}$ (*n*/µL)	11(7-19)	14(12-21)*	37(19-134)*†	131(56-271)*†‡	<0.0001

Data are presented as median (IQR). *p<0.05 vs. CTR; †p<0.05 vs. UA; ‡p<0.05 vs. NSTEMI. Statistical analysis was performed by Kruskal-Wallis (K-W) test and Mann-Whitney *U* test for pairwise comparisons.

Table 3. Immune Inflammation Markers

	UA (*n*=11)	NSTEMI (*n*=10)	STEMI (*n*=26)	*p* (K-W)
MMP-9 (ng/mL)	429(320-460)	446(324-597)	544(466-758)*	<0.01
S100A8/A9 (ng/mL)	7332(4638-9461)	13802(9152-21066)*†	17352(8592-27830)*	<0.05
NGAL (ng/mL)	264(197-317)	327(210-473)	417(312-652)*	<0.05
MPO (ng/mL)	221(152-337)	322(158-443)	389(229-487)*	=0.05
IL-6 (pg/mL)	11.2(9.2-21.1)	30.6(24.5-57.4)*	57.8(22.0-115.9)*	<0.01
TNFα (pg/mL)	1.8(1.3-15.7)	4.6(2.9-7.2)	9.8(2.5-21.8)	0.223
IL-1ß (pg/mL)	2.4(2.2-2.9)	4.2(2.4-7.9)	9.5(3.0-16.7)*	<0.05

Data are presented as median (IQR). *p<0.05 vs. UA. Statistical analysis was performed by Kruskal-Wallis (K-W) test followed by Mann-Whitney *U* test for pairwise comparisons.